

# International Journal of Advance Research in Computer Science and Management Studies

Research Article / Survey Paper / Case Study

Available online at: [www.ijarcsms.com](http://www.ijarcsms.com)

## *A Low-Cost Super Ultra-Wideband Microstrip Antenna with Variable Band-Notch Filtering and an Improved Radiation Pattern for 5G/IoT Applications*

**Dr. Priyanka Bansal<sup>1</sup>**

Professor  
Faculty Of Engineering  
Baba Mastnath University,  
Rohtak(Haryana)-124001, India.

**Shikha<sup>2</sup>**

Research Scholar  
Faculty Of Engineering  
Baba Mastnath University,  
Rohtak(Haryana)-124001, India.

*Abstract: This paper presents a new design of a compact microstrip antenna with variable band-notched filtering characteristics for super ultra-wideband (UWB) applications such as 5G/IoT networks. More efficient radiation patterns and characteristic impedance are accomplished in the proposed structure by producing steps with optimised proper widths and angles in the lower edges of the quasi-square patch antenna and by using a new way of changing the ground plane. Furthermore, omnidirectional low cross-polarized H-plane radiation patterns are achieved in the frequency range of 3-11 GHz. Furthermore, its radiation patterns are enhanced between 11 and 14.5 GHz, and its performance is increased, particularly with tuning capacitors between 14.5 and 20 GHz. Furthermore, its frequency bandwidth with VSWR 2 ranges from 3 GHz to 50 GHz, including 5G networks as well as ultra-wideband (UWB) and super-wideband (SWB) communications. A rectangular slot on the patch is utilised to produce an integrated band-notch filter in the structure to avoid interference with other wireless systems such as wireless local area networks (WLANs), and this specification may be engaged or deactivated by a PIN diode. Furthermore, the centre frequency of the filter can be tuned using only a varactor diode or a variable capacitor and/or by changing the position of the capacitors in the frequency range of about 3.5-6 GHz, rejecting interference from all WLANs and even their lower and upper bands, and nulls in the radiation patterns can be avoided.*

*Keywords: Super Ultra-Wideband, 5G.*

### I. INTRODUCTION

Wireless data traffic is expected to expand 10,000 fold during the next 20 years due to increased use of smartphones, tablets, new wireless devices, and the Internet of Things (IoT). To address this ever-increasing capacity need and to support 5G (5th Generation Networks) requirements more than 10 Gbps peak and edge speeds greater than 100 Mbps for extreme mobile broadband (eMBB) applications, a new spectrum beyond sub-6 GHz frequencies is required. Because of the availability of huge bandwidths at mmWave frequencies, the 5G requirements for eMBB can be addressed with a simple air interface and high dimension phased arrays. mmWave systems must also overcome intrinsic problems like as high penetration loss, increased sensitivity to occlusion, and decreased diffraction. The higher frequencies used for 5G enable higher data transmission across wider channels, resulting in much lower latency as compared to present levels. The Federal Communications Commission (FCC) assigned frequency range 3.1-10.6 GHz for ultra-wideband (UWB) systems in 2002 [1]. Some UWB systems and applications have been introduced in references such as [2-7]. In addition, on July 14, 2016, the US Federal Communications Commission (FCC) enacted new rules for wireless broadband operations above 24 GHz, making the US the first jurisdiction to

make this spectrum available for next generation wireless services. The FCC allocated approximately 11 GHz for flexible, mobile, and fixed use of wireless broadband, including 7 GHz of unlicensed spectrum from 64 to 71 GHz and 3.85 GHz of licensed spectrum designated as a new "upper microwave flexible use" service in three bands: 27.5 to 28.35 GHz, 37 to 38.6 GHz, and 38.6 to 40 GHz. Table 1 depicts a breakdown of the primary frequencies established for use in 5G networks. FR1 will most likely be utilised for initial implementations, with FR2 following. The second graphic shows the FR2 frequency bands of importance. The FCC has also released spectrum from 64 GHz to 71 GHz for future use [6-9]. As we know, wireless sensor networks such as zigbee, LDWA, LoRa, WWAN, and mobile radio networks such as 2G, 3G, 4G, and the upcoming 5G require higher frequency bandwidth, data processing, and machine learning for optimal performance. Furthermore, there are several uses and needs for speedier wireless networks, such as reduced response time (40 times faster).

**Table1.**Proposed5Gfrequenciesindetails

Band	Frequency(MHz)		Type		
FR1	450–6000		Sub-6GHz		
FR2	24250–52600		mm-Wave		
5G NR Band	Band Alias (GHz)	UplinkBand (GHz)	DownlinkBand (GHz)	Bandwidth(GHz)	Type
n257	28	26.5–29.5	26.5–29.5	3	TDD
n258	26	24.25–27.5	24.25–27.5	3.25	TDD
n260	39	37–40	37–40	3	TDD

Printed monopole antennas are more commonly used in UWB applications since they meet all essential criteria. Although a considerable number of tiny UWB antennas have been constructed in recent years [9- 14], their upper frequencies are less than 10.6 GHz. Furthermore, their omnidirectional H-plane radiation patterns are confined to 3 to 10 GHz. For example, in [12], a novel super-wideband (SWB) antenna with an optimised feed is presented, and its bandwidth is from 1.05 to 32.7 GHz with VSWR 2, despite the antenna's partly large size, and the antenna's H-plane radiation pattern in the frequency range is not only non-omnidirectional but also has high sensitivity. However, because to their higher power density, many narrowband wireless communication systems in the UWB spectrum, such as WLANs (5.15-5.825), can cause interference with other communication systems, particularly UWB ones. As a result, UWB systems must be capable of interference rejection, and a traditional solution is to add a filter to the system. However, designing a filter increases the system's size, is expensive, and necessitates the use of modern optimisation techniques. As a result, designers must experiment with various design methodologies, which is time-consuming [13, 14].

A slit in the radiation patch is constructed and employed in this paper to overcome the interference problem, as shown in Fig. 1. Some strategies have been researched and used in references [15-17]. These strategies include etching shaped slots in the feed line or radiation patch [18, 19], employing rectangular split-ring resonators [20], using parasitic components [7], and so on. Nonetheless, in SWB systems such as [12], band-rejection is overlooked. Horizontal surface currents (relative to the x axis) flow in the lower border of the radiation patch and are larger than vertical surface currents in a square monopole antenna like [11], reducing bandwidth and degrading radiation performance at higher frequencies (especially > 10 GHz). In this study, a balance between the components of vertical and horizontal surface currents on the patch is produced for improved performance by altering and optimising the antenna construction. In other words, enhanced radiation patterns in the super UWB (SUWB) frequency band have been obtained by altering the patch, ground plane, and feed line. By cutting aperture slots.

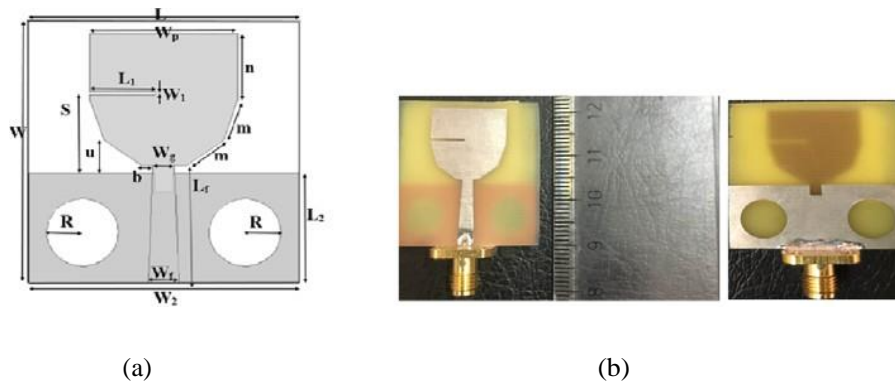


**Figure 1.** Geometry of the proposed antenna; (a) View of the proposed antenna. (b) Top/bottom prototype of the proposed antenna.

Unwanted current distributions are reduced on the ground plane, and improved radiation patterns are obtained up to 14 GHz. Finally, the proposed optimised antenna is modelled using Ansys HFSS software on FR4 and Rogers TMM4 substrates before being constructed and measured. The proposed antenna has a bandwidth of 3 to 50 GHz. Radiation patterns are omnidirectional from 3 to 11 GHz, and higher radiation pattern performance can be attained between 11 and 14 GHz using tuning capacitors and up to 20 GHz with optimisation and modification (for example, a 2 pF tuning capacitor in 15 GHz). Furthermore, the centre frequency of the band-notched filter can be changed from 3.5 to 6 GHz by modifying the structural shape and/or variable capacitor.

## II. ANTENNA CONFIGURATION AND DESIGN

The shape of the proposed antenna is depicted in Figure 1. The antenna is planned, simulated, and fabricated on a FR-4 substrate with dimensions of 30 mm 30 mm, permittivity ( $\epsilon_r$ ) of 4.4, and thickness ( $h$ ) = 1.6 mm. Regardless, the antenna is also modelled on a Rogers TMM4 substrate for better comparison to low loss dielectric substrates. The design procedure and antenna properties are fully explained in this section.  $W = 30, L = 30, W_2 = 30, L_2 = 13, W_1 = 0.4, W_f = 3.4, L_f = 13.95, W_g = 2.4, R = 4, S = 9.3, u = 3.93, b = 1.33, n = 7.79, m = 5.07, W_p = 16.4, L_1 = 7.3$ .

### Antenna Design and Matching

The antenna layout and improvement procedure, as well as the VSWR findings of the suggested antennas, are depicted in Figs. 2 and 3, respectively. The primary antenna, depicted in Fig. 2(a), has a square-like patch with a straight feed line and a defective ground plane. A tiny slot (2 mm 2.2 mm) is drilled into the ground plane to improve impedance matching and radiation performance. Because the antenna's shape is comparable to that of a disc microstrip, the lowest frequency of the antenna may be determined roughly using Equation (1) [17]:

$$fL = 7.2 / ((1 + \epsilon_r + \epsilon_p) k) \text{ GHz} \quad (1)$$

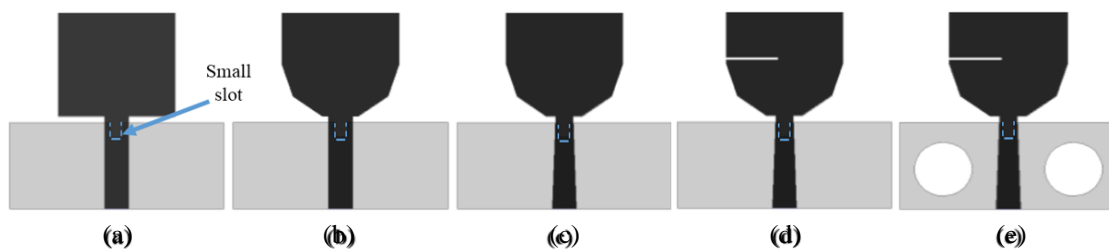


**Figure 2.** Proposed antenna design process.

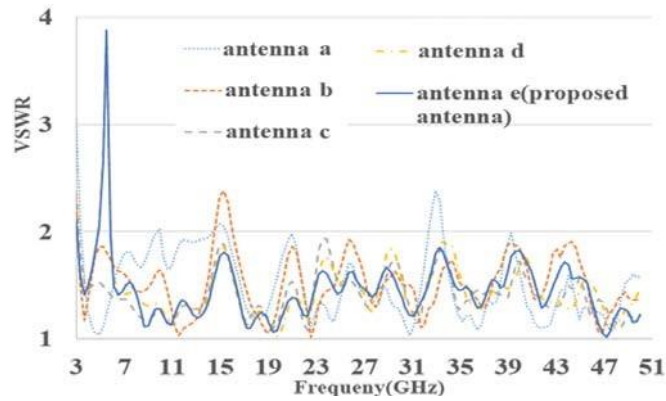


**Figure 3.** Simulated results of VSWR for the antenna models.

This can be a decent estimate for the primary design. In Equation (1),  $k = 1.15$ ,  $l$  is the patch's height,  $p$  is the air gap between the patch and the ground plane, and  $r$  is the effective radius of an analogous cylindrical monopole antenna. The bandwidth of the primary antenna (antenna a) ranges from 3.4 to 10 GHz with a VSWR of 2. A rectangular slot in the patch's bottom edge can be used to balance the components of horizontal and vertical currents [21].

In this study, as illustrated in Fig. 2, trapezoidal and triangular pieces are merged in the patch's edges to form the antenna construction. As a result, the bandwidth of the second structure in Fig. 1 (antenna b) is extended to 11 GHz. As can be observed in Fig. 3, the value of VSWR has decreased. A tapered feed line is replaced by a rectangle one in the third construction (antenna c). The latter arrangement can achieve good impedance matching throughout the entire frequency (3 to 50 GHz). In addition, the fourth structure (antenna d) is created by carving a rectangular slot on the patch in order to eliminate a typical narrowband WLAN signal. Finally, the fifth structure (antenna e) is designed to increase radiation performance and VSWR by constructing two circular apertures on the ground plane. Subsections 2.2 and 2.3 have been expanded to provide a more detailed explanation and details of the final antennas (d and e).

### Band-Notched Characteristics of the Antenna

Various effects of rectangular slot diameters are examined in this section utilising (varying) capacitors. In addition, the construction of a band-notch filter for the antenna structure is explained. The band-notched characteristic reduces bandwidth. For example, in [11], the VSWR of the suggested antenna without a band-notched filter is approximately from 2.4 to 12.5 GHz, whereas adopting a band-notched filter reduces the bandwidth to 2.4-11.2 GHz. The antenna being used in this case has an ultra-wideband, and inserting and/or altering a band-notched filter has no effect on frequency bandwidth. As a result, the exact size and positioning of the band-notched filter's rectangular slot must be determined and set precisely in order to have a beneficial impact across the whole frequency range of the Super SUWB antenna.

WLAN systems operate at frequencies ranging from 4.85 to 5.83 GHz, as previously stated. In addition, Equation (2) defines the centre frequency of the band-notched antenna ( $f_{notch}$ ), where  $c$  is the speed of light in free space,  $r$  is the dielectric constant, and  $L_1$  is the length of the rectangular slot.  $L_1$  is roughly a quarter wavelength at the centre frequency of the band-notched structure and can be computed as [17]:  $L_2 = c / (2 f_{notch} ((r + 1) / 2))$  (2)

The substrate that was chosen for simulation and production is FR4. Figure 4 displays the vertical VSWR findings of the final simulated antenna that has various rectangular slot diameters ( $L_1$ ,  $W_1$ , and  $S$ ). As shown in Fig. 4(a), the bandwidth and centre frequency of the band-notched feature can be modified by adjusting  $L_1$  ( $W_1 = 0.4$  mm,  $S = 9.3$  mm). Furthermore, Fig. 4(b) shows that  $W_1$  ( $L_1 = 7.3$  mm,  $S = 9.3$  mm) and  $S$  ( $L_1 = 7.3$  mm,  $W_1 = 0.4$  mm) define the lowest and highest frequencies of the band-notched filter, respectively. In another arrangement, a varactor diode or variable capacitor or otherwise

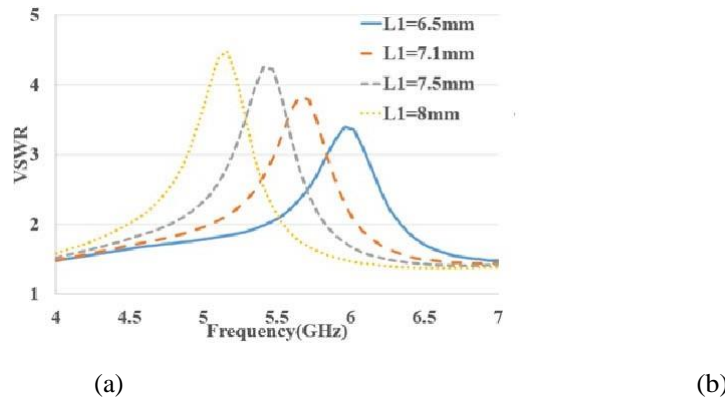


**Figure4.** Effects of slot parameters varying ( $L_1$ ,  $W_1$ , and  $S$ ) on FR4 substrate.

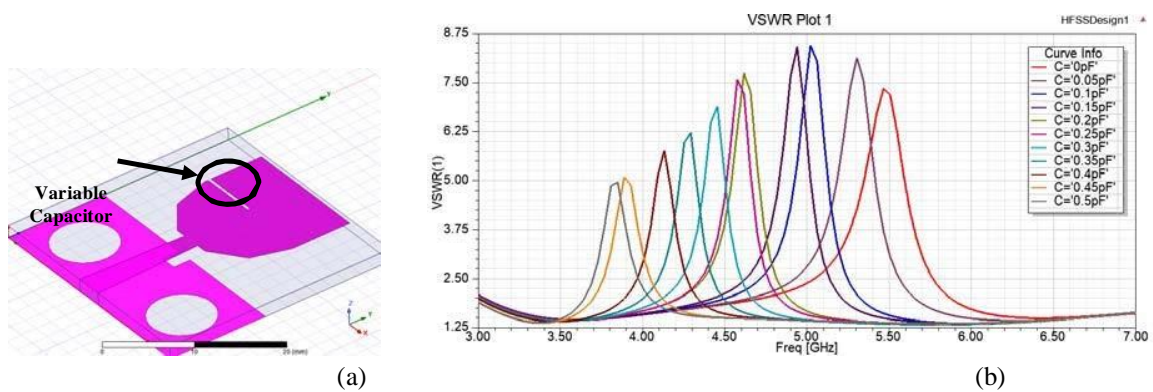


**Figure5.** Effects of adding and changing variable capacitor to the antenna; (a) antenna structure, (b) simulated results on Rogers TMM4 substrate.

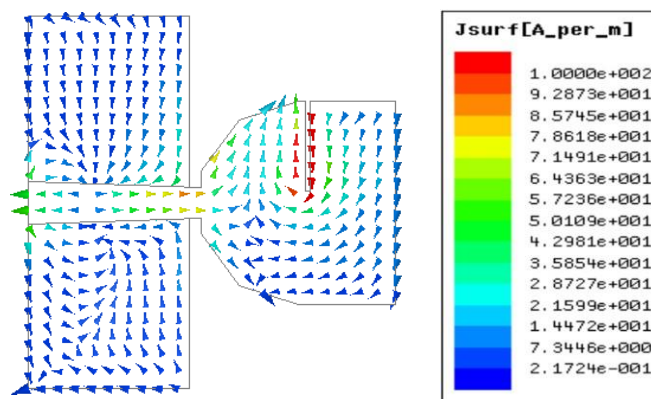


**Figure6.** Simulated current distribution at 5.49GHz.

Capacitive slots are added in the patch antenna gap, and the capacitor value is increased from 0 to 2 pF. The findings are given in Fig. 5 and show that the centre frequency of the antenna's band-notch filter may be easily modified by using a variable capacitor. The final measurements of the rectangular slot band-notched filter are as follows:  $L_1 = 7.3$  mm,  $W_1 = 0.4$  mm, and  $S = 9.3$  mm. Fig. 6 depicts the surface distribution of current of the band-notched filter at  $f_{notch} = 5.49$  GHz. As can be seen, the current arrangement at 5.49 GHz is primarily towards the rectangle.

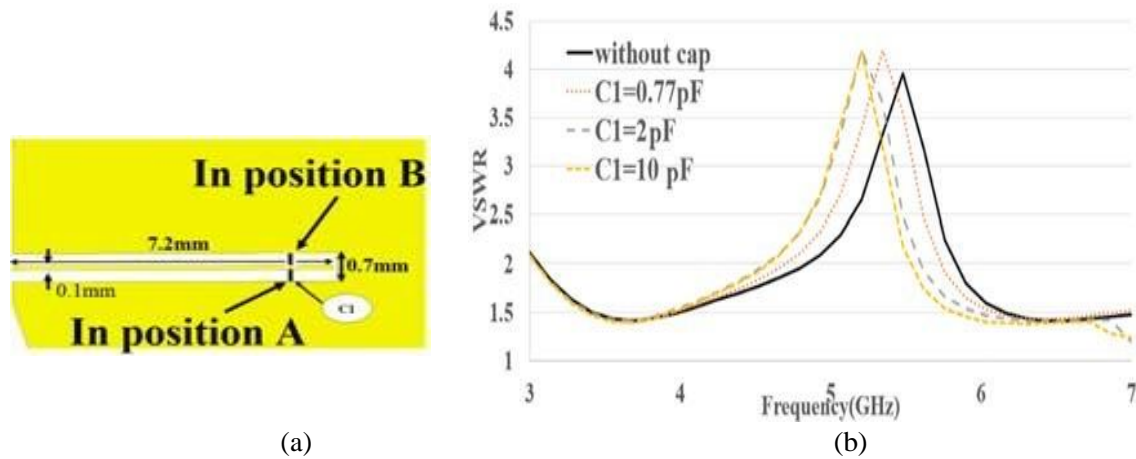


**Figure 7.**(a) Capacitor and microstrip line added to the rectangular slot;(b) Measured VSWR for different values of  $C_1$ .

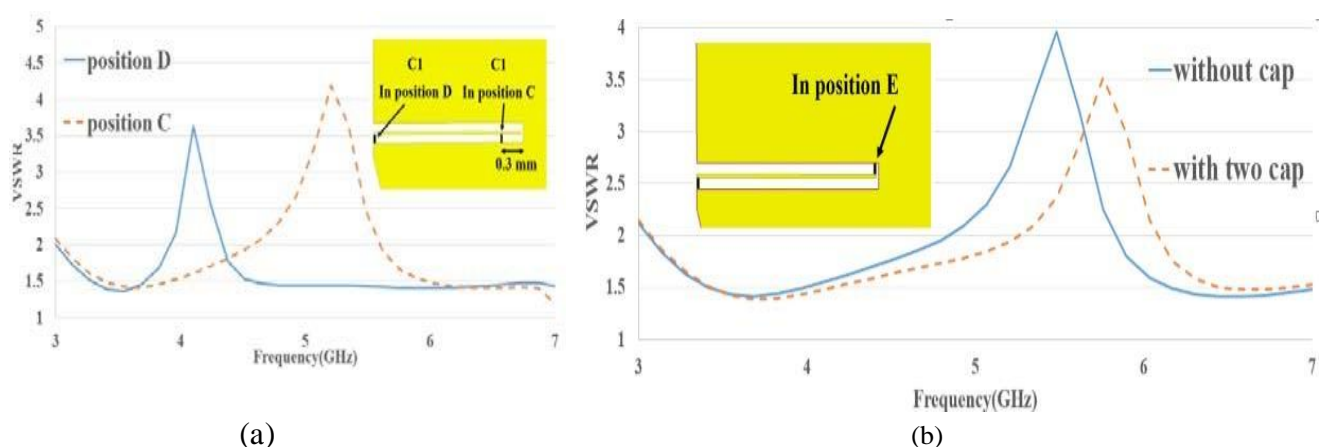


**Figure 8.**(a) Measured VSWR for position C, D ( $C_1 = 2$  pF), (b) Measured VSWR with two capacitors and a microstrip line.

Slot, and it disables excited surface currents close to the band-notched filter's central frequency. In addition, by inserting a PIN diode switch within the rectangular slot of the proposed antenna, the band-notched filter may be switched on and off. When the switch is turned off, the antenna has no band-notched functionality; when turned on, the antenna becomes a super UWB antenna with variable frequency band-notched performance. In a further arrangement and to alter the structure's band-notched filter, a microstrip line or capacitive slot will be placed in the rectangular slot, and then a capacitor ( $C_1$ ) at position A, as shown in Fig. 7(a). The capacitor's value is then adapted, and the centre frequency of the band-notched filter is changed, as shown in Fig. 7(b). When the capacitor is mounted in position B, its capacity to tune the centre frequency of the band-notched filter corresponds to that of the capacitor in position A. likewise, as shown in Fig. 8(a), shifting the capacitor location (2 pF for positions C and D) affects the centre frequency of the structure's band-notched filter. According to references [22-27], if another capacitor is added and positioned in position E, the frequency tuning criteria of the structure's band-notched screen will be boosted and will cover greater and longer frequency ranges (Fig. 8(b)). In this example, the capacitor values and a greater distance in between the capacitors are efficient for an expanded frequency tuning range, which is virtually between 3.5 and 6.087 GHz.

Other microstrip lines and capacitors can be added to increase and improve the frequency tuning range. In this situation, each capacitor has its own frequency tuning effect. For example,  $C_1$  is dominant for tuning, but  $C_2$  and  $C_i(s)$  are better suited for modifying. Table 2 also depicts comparisons between the proposed antenna and other antennas in references with different features. The suggested antenna features a large bandwidth tuning capability, superior performance, and a small dimension. In

addition, better and more stable H-plane radiation patterns in the frequency range of 3 GHz to 15 GHz with tuning skills as well as modifications can be generated (for example, with a 2 pF tuning capacitor or varactor diode in 15 GHz, previously described). Although the gap may not be large enough to insert an SMD capacitor or diode, this problem can be responded to by employing an alternate design (Fig. 5(a)) or die technology. Figure 9 depicts modelled H-plane and E-plane radiation patterns in the frequency range of 3-14 GHz.

**Table2.** Comparison between the proposed antenna and many antenna.

Ref	Size(m <sup>3</sup> )	Bandwidth	Planar	Device used	$\epsilon_r$	Band-notched filter center frequency (GHz)	Tunable	Pattern Stability (GHz)
[27]	80×80×20	UWB	No	Capacitor	2.33	4.8–7.4	no	Upto10
[28]	100×100×19	UWB	No	Diode	3.2	4.5–6.1	no	Upto8
[29]	77×80×0.76	UWB	Yes	Diode	3.5	5.2–6.1	no	Upto5.72
[30]	30×30×0.8	3.1–18	Yes	Diode	4.4	2.7–7.1	no	Upto10
<b>The proposed antenna</b>	30×30×1.6	3–50 simulation	Yes	Capacitor/ Diode	4.4	3.5–6.087	Yes	Upto14
		3–40 measurement		Capacitor/ Diode				

H-plane patterns have been significantly improved, and E-plane patterns are now unidirectional. As shown in Figs. 9 and 13, uniform and optimised H-plane radiation patterns can be obtained up to 20 GHz (with tuning capacitor adjustment and/or tuning). Cross-polarization frequencies grow over 14 GHz due to a surge in orthogonal currents on the surface.

**Radiation Patterns**

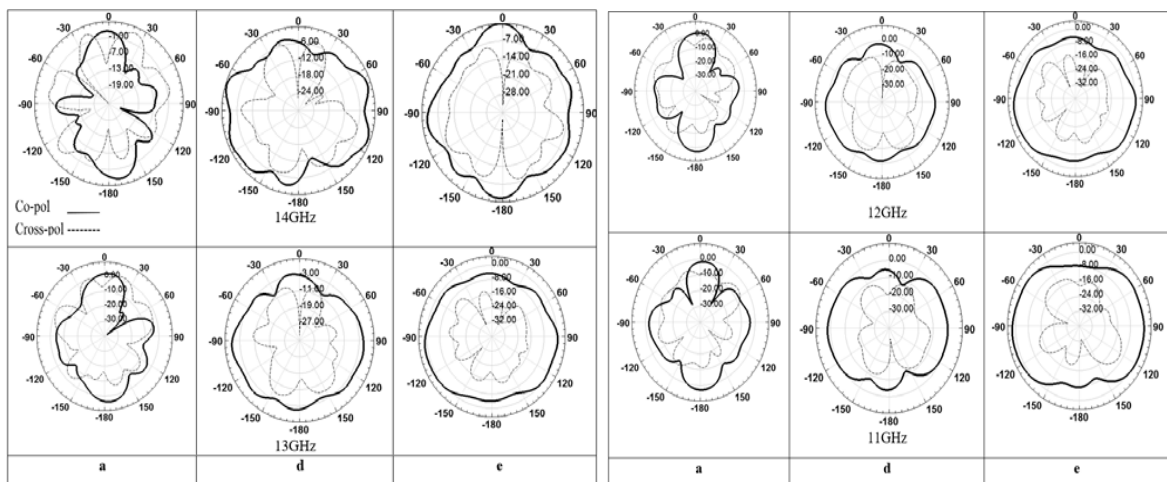


**Figure 9.** Simulated H-plane radiation patterns of antennas a, d and e at 4 different frequencies.

The ground plane shape decides the coupling effects between the patch and the base plane, which impacts UWB antenna performance. Most papers, such as [18] and [24], solely use defective ground structures (DGSs) and develop ground plane slots to increase bandwidth. Yet, a few articles study and investigate the effects of ground planes. The size and geometric features of the ground plane have been discovered to affect radiation patterns [25-35]. Moreover, radiation patterns only rise in the frequency

range of 3-10 GHz in references. A UWB antenna with two ground planes (32 15 mm<sup>2</sup> and 70 15 mm<sup>2</sup>) is used in [25], for example, and L-shaped slots have been established on the leading edges of the ground planes. The radiation patterns of antennas with large planes of ground and slots are identical. The primary distinction is that the antenna with slots in the ground plane produces smaller cross-polarized electromagnetic fields at lower frequencies. In any event, the electromagnetic patterns of the antennas have been adjusted for UWB applications. Still, there are certain issues.

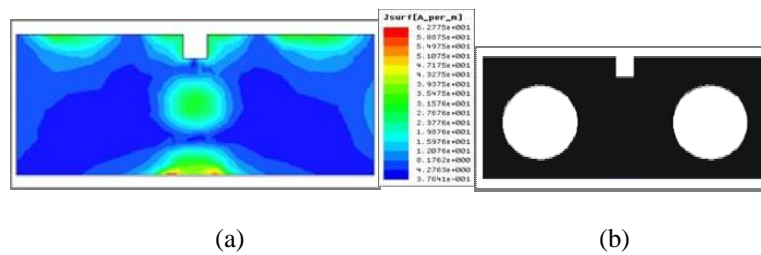


**Figure 10.** (a) Simulated current distributions for SWB antenna at 12 GHz.  
(b) Geometry of the modified ground of SWB antenna.

Not investigated: first, the radiation patterns of the antenna with very small ground planes (32 mm 15 mm with slot), and second, the reasons for grabbing places of the slots in ground planes.

The radiation patterns and gain of the proposed antenna can be seen in the following figures in this section. Figure 9 displays the simulated H-plane radiation patterns of antennas (a), (d), and (e) at four different frequencies. As can be seen, changing the patch and feed line changes the H-plane radiation patterns of antenna (d). In addition, Fig. 10(a) illustrates the simulation of the surface current distribution for the ground plane of antenna (d) at 12 GHz. Surface current amplitudes are smaller in some regions when compared to others as well. To improve radiation properties, two circular holes with a radius of  $R = 4$  mm were eliminated from the ground plane (Figs. 1 and 10(b)). Fig. 9 illustrates that by cutting two circular apertures from the ground plane, antenna (e) has a more omnidirectional and wider frequency range than antenna (d). Furthermore, the bandwidth of the modified antenna is substantially wider than that of the other antennas listed in the references [3-9]. The antenna additionally has a flexible band-notched filters feature. In summary, an antenna with a broader frequency bandwidth, radiation pattern, and variable band-notched filtering characteristic was designed, and H-plane radiation has been raised up to 14 GHz by carving aperture slots in the ground plane. Additionally, as the orthogonal surface currents grow at higher frequencies, the cross-polarized electromagnetic radiation expands.

### III. MEASUREMENT AND SIMULATION RESULTS

The developed antenna appears in Fig. 1(b), and the simulation and measurement results of the proposed antenna are depicted in Figs. 11-15. As can be observed, there is a significant agreement between the simulation and measurement results, with slight variations attributable to the effects of the fabrication process and SMA connector. The proposed antenna's return loss has been evaluated using an Agilent E8363C PNA network analyzer. Figure 12(a) depicts the antenna gain (e). Because the measured VSWR is up to 40 GHz, the antenna is modelled in the frequency range of 3-40 GHz. As can be seen, the gain is tremendous.



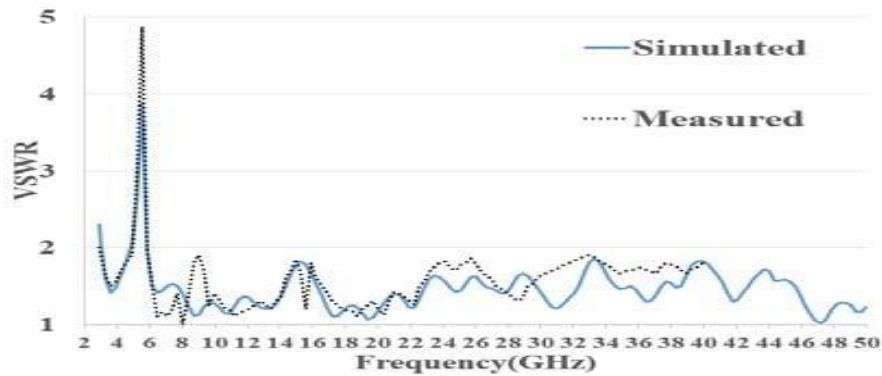


**Figure 11.** Simulated and measured VSWR of the proposed antenna.

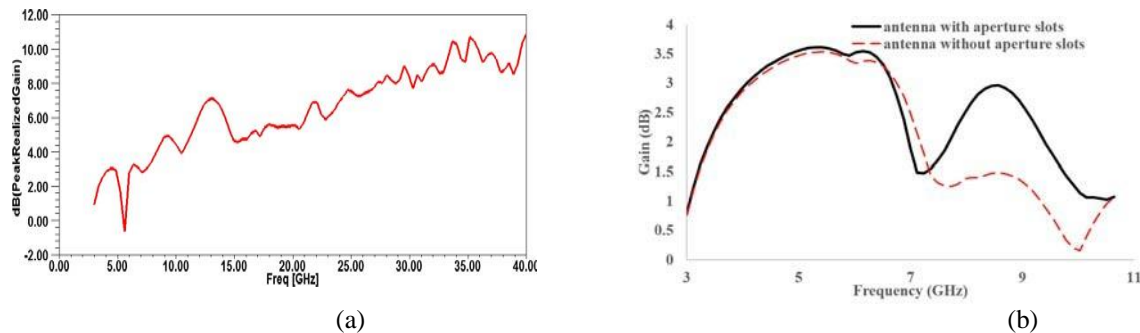


**Figure 12.** (a) Simulated peak gain of the SWB antenna with band-notched. (b) Gain of the proposed antenna without band-notched (with aperture slots and without aperture slots).

#### IV. CONCLUSION

A minuscule super ultra-wideband antenna with variable band-notched filtering capabilities has been presented. The patch's improved structure, with its 50-tapered feed line and engraved slots on the ground plane, offers a wider impedance bandwidth (3 to 50 GHz) and lower cross-polarised and omnidirectional radiation patterns than similar antennas in the literature. This antenna can be used in a very broad frequency range, including a 5G network. The WLAN band has been filtered using a quarter wave slot and capacitors, and the centre frequency of the rejection filter can be set in the patch by using constant and/or variable capacitors. The above method might impact some nulls in radiation patterns. The proposed antenna's small size, best return loss in a complete frequency range, and improved radiation patterns make it a viable contender for UWB and SWB applications. Although this antenna has a simple and economical structure, it is extremely adaptable and efficient, especially when compared to complicated antennas.

#### References

1. First Report and Order in the matter of Revision of Part 15 of the Commission's Rules Regarding Ultra-Wideband Transmission Systems, Released by Federal Communications Commission, ET-Docket 98-153, 2002.
2. Liu, L.-L., et al., "A compact band-notch ultra-wideband antenna," 2017 International Workshop on Electromagnetics: Applications and Student Innovation Competition (iWEM), IEEE, 2017.
3. Ali, J., et al., "Ultra-wideband antenna design for GPR applications: A review," International Journal of Advanced Computer Science and Applications, Vol. 8, No. 7, 392–400, 2017.
4. Awais, Q., et al., "A novel dual ultrawideband CPW-fed printed antenna for internet of things (IoT) applications," Wireless Communications and Mobile Computing, Vol. 2018, 2018.
5. Cicchetti, R., E. Miozzi, and O. Testa, "Wideband and UWB antennas for wireless applications: A comprehensive review," International Journal of Antennas and Propagation, Vol. 2017, 2017.
6. Ahmed, F., N. Hasan, and M. H. M. Chowdhury, "A compact low-profile ultra wideband antenna for biomedical applications," International Conference on Electrical, Computer and Communication Engineering (ECCE), IEEE, 2017.
7. Franchina, V., et al., "A UWB antenna for X-band automotive applications," 2016 IEEE International Symposium on Antennas and Propagation (APSURSI), IEEE, 2016.
8. Kundu, S. and S. K. Jana, "Leaf-shaped CPW-fed UWB antenna with triple notch bands

- for ground penetrating radar applications," *Microwave and Optical Technology Letters*, Vol. 60, No. 4, 930–936, 2018.
9. *Microwave Journal*, Vol. 62, No. 3, Mar. 2019.
  10. Kazim, J., A. Bibi, M. Rauf, M. Tariq, and O. Owais, "A compact planar dual-band-notched monopole antenna for UWB application," *Microw. Opt. Technol. Lett.*, Vol. 56, No. 5, 1095–1097, Mar. 2014, doi:10.1002/mop.28270.
  11. Liu, H.-W., C.-H. Ku, T.-S. Wang, and C.-F. Yang, "Compact monopole antenna with band-notched characteristic for UWB application," *IEEE Antennas Wirel. Propag. Lett.*, Vol. 9, 397–400, May 2010, doi:10.1109/LAWP.2010.2049633.
  12. Liu, J., K. P. Esselle, S. G. Hay, and S. S. Zhong, "Compact super wide band asymmetric monopole antenna with dual-branch feed for bandwidth enhancement," *Electron. Lett.*, Vol. 49, No. 8, 2013.
  13. Singh, U. and R. Salgotra, "Synthesis of linear antenna array using flower pollination algorithm," *Neural Computing and Applications*, Vol. 29, No. 2, 435–445, 2018.
  14. Gevorkyan, A. V., T. Yu Privalova, and Yu V. Yukhanov, "Radiation characteristics of the low profile dipole antenna," 2018 Progress In Electromagnetics Research Symposium (PIERS — Toyama), 1621–1625, Japan, Aug. 1–4, 2018.
  15. Li, W. T., X. W. Shi, and Y. Q. Hey, "Novel planar UWB monopole antenna with triple band-notched characteristics," *IEEE Antennas Wirel. Propag. Lett.*, Vol. 8, 1094–1098, Oct. 2009, doi:10.1109/LAWP.2009.2033449J.
  16. Ray, K. P. and Y. Ranga, "Ultra wideband printed elliptical monopole antennas," *IEEE Trans. Antennas Propag.*, Vol. 55, No. 4, 1189–1192, 2007.
  17. Gao, P., L. Xiong, J. Dai, S. He, and Y. Zheng, "Compact printed wide-slot UWB antenna with 3.5/5.5-GHz dual band-notched characteristics," *IEEE Antennas Wirel. Propag. Lett.*, Vol. 12, 983–986, 2013.
  18. Choukiker, Y. K. and S. K. Behera, "Modified Sierpinski square fractal antenna covering ultra-wideband application with band notch characteristics," *IET Microw. Antennas Propag.*, Vol. 8, No. 7, 506–512, May 2014, doi:10.1049/iet-map.2013.0235.
  19. Kelly, J. R., P. S. Hall, P. Jardner, and F. Ghanem, "Integrated narrow/band-notched UWB antenna," *Electron. Lett.*, Vol. 46, No. 12, 814–816, Jun. 2010, doi:10.1049/el.2010.3368.
  20. Sarkare, D., K. V. Srivastava, and K. Saurav, "A compact microstrip-fed triple band-Notched," *IEEE Antennas Wirel. Propag. Lett.*, Vol. 13, 396–399, Feb. 2014, doi:10.1109/LAWP.2014.2306812.
  21. Jung, J., W. Choi, and J. Choi, "A small wideband microstrip-fed monopole antenna," *IEEE Microw. Wireless Compon. Lett.*, Vol. 15, No. 10, 703–705, Oct. 2005.
  22. Heon, D. H., H. Y. Yang, and Y. K. Cho, "Tapered slot antenna with band-notched function for ultrawideband radios," *IEEE Antennas Wirel. Propag. Lett.*, Vol. 11, 682–685, 2012.
  23. Tripathi, S., A. Mohan, and S. Yadav, "Hexagonal fractal ultra wideband antenna using Koch geometry with bandwidth enhancement," *IET Microw. Antennas Propag.*, Vol. 8, No. 15, 1445–1450, 2014.
  24. Fereidoony, F., S. Chamaani, and A. Mirtaheeri, "Systematic design of UWB monopole antennas with stable omnidirectional radiation pattern," *IEEE Antennas Wirel. Propag. Lett.*, Vol. 11, 752–755, 2012.
  25. Lu, Y., Y. Huang, H. T. Chattha, and P. Cao, "Reducing ground-plane effects on UWB monopole antennas," *IEEE Antennas Wirel. Propag. Lett.*, Vol. 10, 147–150, 2011.
  26. Ammann, M. J. and M. John, "Optimum design of the printed strip monopole," *IEEE Antennas and Propagation Magazine*, Vol. 47, No. 6, Dec. 2005.
  27. Hu, Z. H., P. S. Hall, J. R. Kelly, and P. Gardner, "UWB pyramidal monopole antenna with wide tunable band-notched behavior," *Electron. Lett.*, Vol. 46, No. 24, 1588–1590, 2010.
  28. Antonino-Daviu, E., M. Cabedo-Fabres, M. Ferrando-Bataller, and A. V. Jimeñez, "Active UWB antenna with tunable band-notched behavior," *Electron. Lett.*, Vol. 43, No. 18, 959–960, 2007.
  29. Jeong, W.-S., D.-Z. Kim, W.-G. Lim, and J. W. Yu, "Tunable band notch ultra wideband planar monopole antenna using varactor," *Microw Opt. Technol. Lett.*, Vol. 51, No. 12, 2829–2832, 2009.
  30. Aghdam, S. A., "A novel UWB monopole antenna with tunable notched behavior using varactor diode," *IEEE Antennas Wirel. Propag. Lett.*, Vol. 13, 1243–1246, 2014.
  31. Awad, N. M. and M. K. Abdelazeez, "Multislot microstrip antenna for ultra-wideband applications," *Journal of King Saud University-Engineering Sciences*, Vol. 30, No. 1, 38–45, 2018.
  32. Khattak, M. I., et al., "Hexagonal printed monopole antenna with triple stop bands for UWB application," *Mehran University Research Journal of Engineering and Technology*, Vol. 38, No. 2, 335–340, 2019.
  33. Li, B., Z.-H. Yan, and T.-L. Zhang, "Triple-band slot antenna with U-shaped open stub fed by asymmetric coplanar strip for WLAN/WiMAX applications," *Progress In Electromagnetics Research*, Vol. 37, 123–131, 2013.
  34. Rahayu, Y. and I. R. Mustofa, "Design of 22 MIMO microstrip antenna rectangular patch array for 5G wireless communication network," 2017 Progress In Electromagnetics Research Symposium — Fall (PIERS — FALL), 2679–2683, Singapore, Nov. 19–22, 2017.
  35. Khattak, M. I., et al., "Elliptical slot circular patch antenna array with dual band behaviour for future 5G mobile communication networks," *Progress In Electromagnetics Research*, Vol. 89, 133–147, 2019.